ACS OMEGA

Article

Cite This: ACS Omega 2018, 3, 12501−12504

http://pubs.acs.org/journal/acsodf

New Lutetium Oxide: Electrically Conducting Rock-Salt LuO Epitaxial Thin Film

Kenichi Kaminaga,[†,‡] Daichi Oka,[∥] Tetsuya Hasegawa,[†] and Tomoteru Fukumura*[,‡,§,∥]

[†]Department of Chemistry, The University of Tokyo, Tokyo 113-0033, Japan

[‡]WPI-Advanced Institute for Materials Research and Core Research Cluster, and [§]Center for Spintronics Research Network, Tohoku University, Sendai 980-8577, Japan

[∥]Department of Chemistry, Tohoku University, Sendai 980-8578, Japan

Supporting Information

ABSTRACT: C-rare earth structure lutetium sesquioxide Lu_2O_3 has been recognized as a high-k widegap insulator with closed shell Lu^{3+} ions. In this study, rock-salt structure lutetium monoxide LuO with unusual valence of Lu^{2+} ($4f^{14}5d^1$), previously known as the gaseous phase, was synthesized as an epitaxial thin film by the pulsed laser deposition method. In contrast with transparent and highly insulating Lu_2O_3, LuO possessed a dark-brown color and high electrical conductivity concomitant with strong spin−orbit coupling as a manifestation of Lu 5d electron carriers.

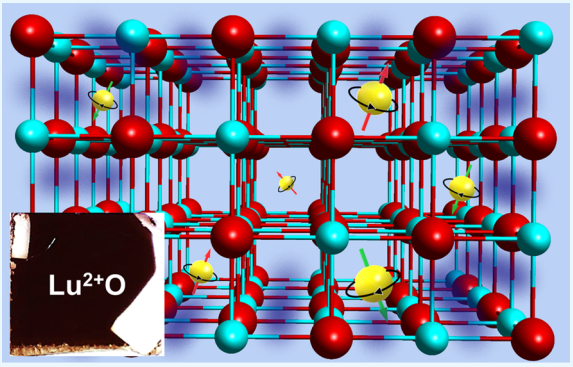

INTRODUCTION

Among binary lutetium oxides, only Lu_2O_3 is the stable solid phase with closed shell trivalent Lu ions,[1] possessing a strong insulating behavior owing to its large band gap (5.8 ± 0.1 eV).[2−4] On the other hand, lutetium monoxide LuO has existed only as a gaseous phase[5−7] such as various rare earth monoxides with divalent cations (except EuO) because of its largely positive Gibbs formation energy of the solid phase.[1,8] However, various rock-salt type rare earth monoxides were recently synthesized in the form of epitaxial thin films owing to nonequilibrium kinetic growth of the pulsed laser deposition method. For example, YO is a narrow gap semiconductor,[9] SmO is a heavy fermionic metal,[10] and LaO is a superconductor.[11] In this study, we report the first synthesis of rock-salt type LuO epitaxial thin films with unusual valence of Lu^{2+} (Lu^{2+}: $[Xe]4f^{14}5d^1$). In stark contrast with high-k insulator Lu_2O_3,[2−4] LuO exhibited a narrow band gap and high electrical conduction with a strong spin−orbit interaction originating from its 5d electron carriers.

EXPERIMENTAL SECTION

LuO epitaxial thin films were deposited by the pulsed laser deposition method. The Lu_2O_3 polycrystalline pellet sintered at 1400 °C was used as a target. The thin films were grown at 300 °C on $CaF_2(001)$ (a = 5.4630 Å) substrates using KrF excimer laser (λ = 248 nm) with an energy density of 1.6 J/cm^2 and a repetition ratio of 15 Hz. Ar + 1% O_2 mixed gas was supplied during the deposition to keep oxygen partial pressure P_{O_2} of 6 × 10^{-10} Torr measured with a quadrupole mass analyzer. Reflection high energy electron diffraction during deposition was in situ monitored to confirm the streak pattern of the thin films. The film surface was in situ capped with an AlO_x layer at room temperature to prevent oxidation.The typical film thickness was approximately 150 nm. From X-ray reflectivity measurement of a referential sample, thickness of the LuO layer and the Lu_2O_3 layer was estimated to be approximately 105 and 40 nm, respectively. The Lu_2O_3 thin film on $CaF_2(001)$ substrates was also deposited as a reference for the absorption spectrum and quantitative analysis by X-ray photoelectron spectroscopy (XPS). θ−2θ X-ray diffractions (XRD) and two-dimensional reciprocal space mapping (RSM) were measured with Cu Kα_1 radiation. XPS combined with Ar^+ sputtering was measured using a monochromated Al Kα source to evaluate ionic valence, where the XPS peak positions were calibrated by the C 1s peak position (284.8 eV). The absence of the impurity element was confirmed by XPS (Figure S1). Absorption spectra were obtained from transmittance and reflectance. Resistivity and the Hall effect under out-of-plane magnetic field were measured using a Hall bar-shaped sample with 1 mm width and 3 mm length to evaluate carrier density and mobility from 2 to 300 K.

Received: August 17, 2018
Accepted: September 19, 2018
Published: October 3, 2018

DOI: 10.1021/acsomega.8b02082
ACS Omega 2018, 3, 12501−12504

RESULTS AND DISCUSSION

Figure 1a shows the θ–2θ XRD pattern of the LuO thin film. Two peaks at 2θ = 36.952° and 78.943° corresponded to the

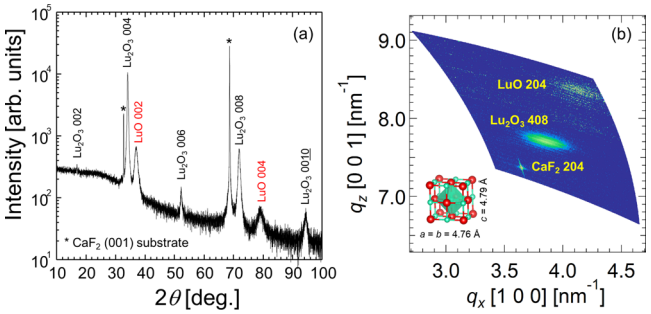

Figure 1. (a) θ–2θ XRD pattern for the LuO thin film on the CaF_2(001) substrate. (b) RSM around the 204 diffraction peak of the CaF_2 substrate, the 204 diffraction peak of the LuO thin film, and the 408 diffraction peak of the cubic Lu_2O_3 film. The inset shows the rock-salt structure of LuO. The structure was drawn by the VESTA program.[23]

rock-salt structure LuO 002 and 004 diffractions, respectively. In addition, cubic Lu_2O_3 00*n* peaks were observed as a result of surface oxidation of LuO similar to the Y_2O_3 surface layer of the YO thin film,[9,12] in which Lu_2O_3 002, 006, and 00$\underline{10}$ forbidden peaks were generated because of oxygen vacancies. Figure 1b shows a two-dimensional RSM of the same LuO thin film as that in Figure 1a. Both the LuO thin film and the cubic Lu_2O_3 layer were fully relaxed and epitaxially grown on the CaF_2 substrate with the epitaxial relationships of LuO [001]||CaF_2 [001] and Lu_2O_3 [001]||CaF_2 [001], respectively. The lattice constants of LuO were $a = b = 4.76$ Å and $c = 4.79$ Å (inset of Figure 1b). The ionic radius of Lu^{2+} in LuO was evaluated to be 0.984 Å from the cube root of the cell volume. This value is slightly smaller than the ionic radius of Lu^{2+} (1.02 Å) calculated from the empirical formula[14] with the Shannon's ionic radius of 6-coordinated Lu^{3+},[13] possibly because of the spatially extended 5d orbital in Lu^{2+} in comparison with the 4f orbital in Lu^{3+}.[15]

Figure 2 shows Lu 4f XPS spectra for LuO and Lu_2O_3 thin films. The XPS spectrum of the Lu_2O_3 thin film was composed of dominant Lu^{3+} peaks, small Lu^0 peaks, plasmons peak, and O 2p peak (Figure 2b), in which the Lu^0 $4f_{7/2}$ peak position (6.5 eV) was consistent with the previous study.[16,17] For LuO thin films, the Lu^{2+} $4f_{7/2}$ peak at 8.0 eV was dominant and located between the Lu^{3+} $4f_{7/2}$ peak at 8.3 eV and the Lu^0 $4f_{7/2}$ peak at 6.5 eV (Figure 2a). The composition was determined to be $Lu_1O_{0.90}$ from the areal intensity ratio of Lu $4d_{5/2}$ and O 1s peaks in the LuO thin film, taking into account the inelastic mean free paths obtained from the TPP-2M predictive equation (see the Supporting Information).[18] The presence of oxygen vacancies in the LuO thin film was consistent with electron carrier conduction in the LuO thin film as described below.

The inset of Figure 3 shows photographs of LuO and Lu_2O_3 thin films. In contrast with the bluish transparent Lu_2O_3 thin film, the LuO thin film possessed dark-brown color as a result of its visible light absorption. Figure 3 shows absorption spectra of LuO and Lu_2O_3 thin films. Lu_2O_3 showed sharp absorption edge with negligible in-gap absorption. On the other hand, the LuO thin film showed a significant and broad visible absorption. The spectral shape shows remarkable

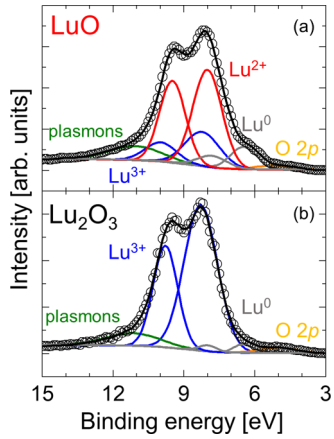

Figure 2. Lu 4f XPS spectra for (a) LuO and (b) Lu_2O_3 films on CaF_2(001) substrates after Ar^+ etching (open symbol). Fitting curves (solid curve) and the deconvoluted Lu^0 (gray), Lu^{2+} (red), Lu^{3+} (blue), the plasmons (green), and O 2p (yellow) spectra are also shown.

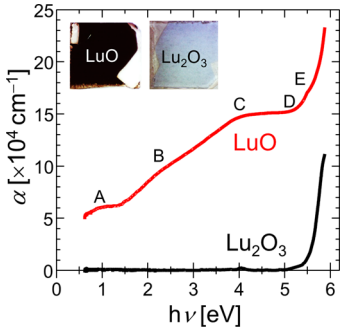

Figure 3. Absorption spectra of the LuO thin film and the Lu_2O_3 film. Inset shows photographs of LuO and Lu_2O_3 films. The indices (A–E) are explained in text.

resemblance with that of the YO thin film[9] and those of Yb monochalcogenides (Yb*X*, *X* = S, Se, and Te) thin films.[19] As indicated in Figure 3, the characteristic absorption energies could be attributed to Lu 4f → Lu 5d t_{2g} transition (A), Lu 4f → Lu 5d e_g transition (B), O 2p → Lu 5d t_{2g} transition (D), and O 2p → Lu 5d e_g transition superposed with intergap absorption of the Lu_2O_3 surface oxidation layer (E). A kink at around 4 eV (C) was similar to that in the YO thin film,[9] in spite of the unknown origin. The spectral resemblance between LuO and YO is caused by similar d^1 electronic configuration of Lu^{2+} with Y^{2+}.

Figure 4a–c shows temperature dependence of the electrical conductivity, the carrier density, and the mobility for the LuO thin film. The temperature dependence of conductivity in the LuO thin film showed a metallic behavior (Figure 4a). The carrier polarity was n-type, probably originated from 5d electrons of Lu^{2+} and oxygen vacancies serving as an electron donor. The carrier density and the mobility were insignificantly changed for 2–300 K, and those at 300 K were 7.4×10^{20} cm^{-3} and 0.46 cm^2/V s, respectively (Figure 4b,c), which were approximately the same as those of metallic YO thin films.[9] The carrier density was extremely small, assuming fully itinerant 5d electrons from Lu^{2+}, estimated to be the carrier density of 3.7×10^{22} cm^{-3}, possibly caused by strong electron correlation between the 5d electrons. Figure 4d shows temperature dependence of resistivity for the LuO thin film

DOI: 10.1021/acsomega.8b02082
ACS Omega 2018, 3, 12501–12504

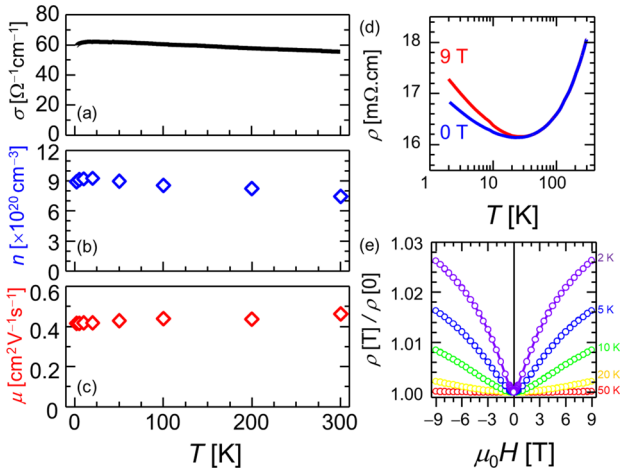

Figure 4. Temperature dependence of (a) conductivity, (b) carrier density, and (c) mobility for the LuO thin film. (d) Temperature dependence of resistivity for the LuO thin film under 0 and 9 T. (e) Isothermal magnetoresistance of the LuO thin film at different temperatures.

at 0 and 9 T. The resistivity of the LuO thin film showed the local minimum at 28 K corresponding to the local maximum of the carrier density (Figure 4b). The resistivity proportional to −log T below 28 K suggests the appearance of the Kondo effect persisting up to 9 T, possibly originated from the presence of oxygen vacancies observed in YO.[9] Figure 4e shows isothermal magnetoresistance of the LuO thin film at 2−50 K. The positive magnetoresistance is thought to be originated from the weak antilocalization effect, indicating strong spin−orbit coupling of the Lu 5d orbital. The maximum magnetoresistance at 2 K and 9 T was +2.6%, which was much larger than that of the YO thin film +0.96%,[9] possibly caused by the larger spin−orbit coupling owing to the heavier Lu element.[20]

CONCLUSIONS

In summary, we synthesized solid phase rock-salt LuO with unusual valence Lu^{2+} in the form of the epitaxial thin film for the first time. The LuO thin film showed strong visible absorption and high electrical conduction, in stark contrast with Lu_2O_3. In addition, the Kondo effect and sizable positive magnetoresistance were observed. The strong spin−orbit interaction in this compound would be useful for spintronic electrodes in heterojunctions like Pt and IrO_2.[21,22]

ASSOCIATED CONTENT

Supporting Information

The Supporting Information is available free of charge on the ACS Publications website at DOI: 10.1021/acsomega.8b02082.

PDF data, discussion of quantitative analysis of the LuO thin film, and typical XPS spectrum for the LuO(001) epitaxial thin film (PDF)

AUTHOR INFORMATION

Corresponding Author

*E-mail: tomoteru.fukumura.e4@tohoku.ac.jp.

ORCID

Kenichi Kaminaga: 0000-0001-7331-7453

Daichi Oka: 0000-0003-2747-9675

Tomoteru Fukumura: 0000-0002-8957-3520

Notes

The authors declare no competing financial interest.

ACKNOWLEDGMENTS

XPS measurement was conducted at Research Hub for Advanced Nano Characterization, The University of Tokyo, under the support of the Nanotechnology Platform by MEXT, Japan (no. 12024046). This work is supported by JST-CREST, JSPS-KAKENHI (nos. 26105002, JP17J05331, 18H03872), and the Mitsubishi Foundation.

REFERENCES

(1) Adachi, G.-y.; Imanaka, N. The Binary Rare Earth Oxides. *Chem. Rev.* **1999**, *98*, 1479−1514.

(2) Perego, M.; Seguini, G.; Scarel, G.; Fanciulli, M. X-ray photoelectron spectroscopy study of energy-band alignments of Lu_2O_3 on Ge. *Surf. Interface Anal.* **2006**, *38*, 494−497.

(3) Darmawan, P.; Lee, P. S.; Setiawan, Y.; Ma, J.; Osipowicz, T. Effect of low fluence laser annealing on ultrathin Lu_2O_3 high-k dielectric. *Appl. Phys. Lett.* **2007**, *91*, 092903.

(4) Darmawan, P.; Lee, P. S.; Setiawan, Y.; Lai, J. C.; Yang, P. Thermal stability of rare-earth based ultrathin Lu_2O_3 for high-*k* dielectrics. *J. Vac. Sci. Technol., B: Microelectron. Nanometer Struct.-Process., Meas., Phenom.* **2007**, *25*, 1203−1206.

(5) Effantin, C.; Bacis, R.; Dincan, J. Rotational analysis of beta system and vibrational analysis of gamma LuO system. *C. R. Seances Acad. Sci., Ser. B* **1971**, *273*, 605.

(6) Cooke, S. A.; Krumrey, C.; Gerry, M. C. L. Rotational spectroscopy of lutetium monoxide. *J. Mol. Spectrosc.* **2011**, *267*, 108−111.

(7) Liu, Z.; Xie, H.; Li, Q.; Qin, Z.; Cong, R.; Wu, X.; Tang, Z.; Fan, H. On the photoelectron velocity-map imaging of lutetium monoxide anion LuO. *J. Chem. Phys.* **2014**, *140*, 034312.

(8) Leger, J. M.; Yacoubi, N.; Loriers, J. Synthesis of rare earth monoxides. *J. Solid State Chem.* **1981**, *36*, 261−270.

(9) Kaminaga, K.; Sei, R.; Hayashi, K.; Happo, N.; Tajiri, H.; Oka, D.; Fukumura, T.; Hasegawa, T. A divalent rare earth oxide semiconductor: Yttrium monoxide. *Appl. Phys. Lett.* **2016**, *108*, 122102.

(10) Uchida, Y.; Kaminaga, K.; Fukumura, T.; Hasegawa, T. Samarium monoxide epitaxial thin film as a possible heavy-fermion compound. *Phys. Rev. B* **2017**, *95*, 125111.

(11) Kaminaga, K.; Oka, D.; Hasegawa, T.; Fukumura, T. Superconductivity of Rock-Salt Structure LaO Epitaxial Thin Film. *J. Am. Chem. Soc.* **2018**, *140*, 6754−6757.

(12) Stellhorn, J. R.; Hosokawa, S.; Happo, N.; Tajiri, H.; Matsushita, T.; Kaminaga, K.; Fukumura, T.; Hasegawa, T.; Hayashi, K. A valence-selective X-ray fluorescence holography study of an yttrium oxide thin film. *J. Appl. Crystallogr.* **2017**, *50*, 1583−1589.

(13) Shannon, R. D. Revised effective ionic radii and systematic studies of interatomic distances in halides and chalcogenides. *Acta Crystallogr., Sect. A: Cryst. Phys., Diffr., Theor. Gen. Crystallogr.* **1976**, *32*, 751−767.

(14) Jia, Y. Q. Crystal radii and effective ionic radii of the rare earth ions. *J. Solid State Chem.* **1991**, *95*, 184−187.

(15) Cox, P. A. *The Electronic Structure and Chemistry of Solids*; Oxford University Press: New York, 1987.

(16) Kaichev, V. V.; Asanova, T. I.; Erenburg, S. B.; Perevalov, T. V.; Shvets, V. A.; Gritsenko, V. A. Atomic and electronic structures of lutetium oxide Lu_2O_3. *J. Exp. Theor. Phys.* **2013**, *116*, 323−329.

(17) Yermolayeva, Y. V.; Tolmachev, A. V.; Korshikova, T. I.; Yavetskiy, R. P.; Dobrotvorskaya, M. V.; Danylenko, N. I.; Sofronov, D. S. Spherical core−shell structured nanophosphors on the basis of

DOI: 10.1021/acsomega.8b02082
ACS Omega 2018, 3, 12501−12504

europium-doped lutetium compounds. *Nanotechnology* **2009**, *20*, 325601.
(18) Tanuma, S.; Powell, C. J.; Penn, D. R. Calculation of electron inelastic mean free paths (IMFPs) VII. Reliability of the TPP-2M IMFP predictive equation. *Surf. Interface Anal.* **2003**, *35*, 268−275.
(19) Narayanamurti, V.; Jayaraman, A.; Bucher, E. Optical absorption in ytterbium monochalcogenides under pressure. *Phys. Rev. B: Solid State* **1974**, *9*, 2521−2523.
(20) Ogasawara, H.; Kotani, A.; Thole, B. T. Lifetime effect on the multiplet structure of 4d x-ray-photoemission spectra in heavy rare-earth elements. *Phys. Rev. B: Condens. Matter Mater. Phys.* **1994**, *50*, 12332−12341.
(21) Kimura, T.; Otani, Y.; Sato, T.; Takahashi, S.; Maekawa, S. Room-temperature reversible spin Hall effect. *Phys. Rev. Lett.* **2007**, *98*, 156601.
(22) Fujiwara, K.; Fukuma, Y.; Matsuno, J.; Idzuchi, H.; Niimi, Y.; Otani, Y.; Takagi, H. 5d iridium oxide as a material for spin-current detection. *Nat. Commun.* **2013**, *4*, 2893.
(23) Momma, K.; Izumi, F. VESTA 3 for three-dimensional visualization of crystal, volumetric and morphology data. *J. Appl. Crystallogr.* **2011**, *44*, 1272−1276.

DOI: 10.1021/acsomega.8b02082
ACS Omega 2018, 3, 12501−12504